TISSUE ENGINEERING: Part C
Volume 20, Number 6, 2014

DOI: 10.1089/ten.tec.2013.0187

Living-Engineered Valves for Transcatheter Venous Valve Repair

Benedikt Weber, MD, PhD,[1–3,5,*] Jérôme Robert, PhD,[1,2,4,5,*] Agnieszka Ksiazek, DVM,[1–3] Yves Wyss, BSc,[1–3] Laura Frese, PhD,[1–3] Jaroslav Slamecka, MSc,[1–3] Debora Kehl, BSc,[1–3] Peter Modregger, PhD,[6,7] Silvia Peter, MSc,[6,8] Marco Stampanoni, PhD,[6,8] Steven Proulx, PhD,[9] Volkmar Falk, MD,[2,3] and Simon P. Hoerstrup, MD, PhD[1–3,5]

Background: Chronic venous insufficiency (CVI) represents a major global health problem with increasing prevalence and morbidity. CVI is due to an incompetence of the venous valves, which causes venous reflux and distal venous hypertension. Several studies have focused on the replacement of diseased venous valves using xeno- and allogenic transplants, so far with moderate success due to immunologic and thromboembolic complications. Autologous cell-derived tissue-engineered venous valves (TEVVs) based on fully biodegradable scaffolds could overcome these limitations by providing non-immunogenic, non-thrombogenic constructs with remodeling and growth potential.

Methods: Tri- and bicuspid venous valves ($n = 27$) based on polyglycolic acid–poly-4-hydroxybutyrate composite scaffolds, integrated into self-expandable nitinol stents, were engineered from autologous ovine bone-marrow-derived mesenchymal stem cells (BM-MSCs) and endothelialized. After *in vitro* conditioning in a (flow) pulse duplicator system, the TEVVs were crimped ($n = 18$) and experimentally delivered ($n = 7$). The effects of crimping on the tissue-engineered constructs were investigated using histology, immunohistochemistry, scanning electron microscopy, grating interferometry (GI), and planar fluorescence reflectance imaging.

Results: The generated TEVVs showed layered tissue formation with increasing collagen and glycosaminoglycan levels dependent on the duration of *in vitro* conditioning. After crimping no effects were found on the MSC level in scanning electron microscopy analysis, GI, histology, and extracellular matrix analysis. However, substantial endothelial cell loss was detected after the crimping procedure, which could be reduced by increasing the static conditioning phase.

Conclusions: Autologous living small-diameter TEVVs can be successfully fabricated from ovine BM-MSCs using a (flow) pulse duplicator conditioning approach. These constructs hold the potential to overcome the limitations of currently used non-autologous replacement materials and may open new therapeutic concepts for the treatment of CVI in the future.

Introduction

Lower extremity chronic venous insufficiency (CVI) displays a global health problem with a substantial socioeconomic impact.[1–3] CVI describes the endpoint of different pathological disorders of the venous system resulting in venous valve insufficiency associated with venous blood reflux, obstruction, stasis, and distal venous hypertension.[1,4] This valvular incompetence can be caused by congenital defects, structural weakness, or abnormally distensible venous walls due to other pathologies.[5] If left untreated, then this results in pain, swelling, significant edema, sclerosis, skin changes, and ulcerations.[1]

For a long time, CVI has been treated conservatively using various compression techniques and devices[6] or—in case of superficial lesions—surgically by ligation of the saphenofemoral junction and stripping of the saphenous vein.[5] In cases of deep vein insufficiency, recently percutaneous transcatheter

[1]Swiss Center for Regenerative Medicine, [2]Division of Surgical Research, [3]Clinic for Cardiovascular Surgery, and [4]Institute for Clinical Chemistry, University Hospital of Zurich, Zurich, Switzerland.
[5]Zurich Center of Integrated Human Physiology, University of Zurich, Zurich, Switzerland.
[6]TOMACT Beamline, Swiss Light Source, Paul Scherrer Institute, Villigen, Switzerland.
[7]School of Biology and Medicine, University of Lausanne, Lausanne, Switzerland.
[8]Institute for Biomedical Engineering, University and ETH Zurich, Zurich, Switzerland.
[9]Institute of Pharmaceutical Sciences, Swiss Federal Institute of Technology, Zurich, Switzerland.
*These authors contributed equally to this work.

valve repair has been investigated as part of first in-man clinical trials using bioprosthetic stented valves. In spite of the initially good performance and the extended anticoagulation protocols, the xenogenic glutaraldehyde-fixed valves showed excessive neo-intimal hyperlasia and fibrotic transformation in the long-term follow-up groups. This resulted in valve incompetence and/or valvular stenosis in up to 90% of patients and—up to now—none of the used prostheses qualified for routine clinical use.[7]

Tissue engineering is aiming at the generation of living autologous substitutes with the potential for remodeling, regeneration, and growth that might overcome the limitations of currently used artificial animal-derived valve substitutes. After biomimetic conditioning of the constructs in the bioreactor, these living constructs are endothelialized in order to provide an antithrombogenic surface that is resistant to thromboembolic complications as reported for current artificial valve prostheses.[8,9] Tissue-engineered valvular substitutes for diseased heart valves have been extensively investigated *in vitro*[10–13] and *in vivo*[14–16] with first-promising results. Besides the field of heart valve disease, also in insufficient venous valves, a living autologous tissue-engineered replacement could restore valvular integrity and function. Importantly, it may hold the potential to overcome the limitations of currently used replacement materials including progressive calcific valvular degeneration as well as clotting activation. However, for a possible future clinical realization of the venous valve tissue engineering concept, these valves would have to fulfill two main criteria: (1) they would have to tolerate the potentially harmful crimping procedure associated with transcatheter valve delivery approaches, and (2) they would have to be fabricated from an easily accessible, ''minimally invasive'' cell source to circumvent the necessity of harvesting intact donor structures.

In a recent investigation[14] we created tissue-engineered heart valves (TEHVs) from bone-marrow-derived mesenchymal stem cells as well as blood-derived endothelial progenitor cells. These TEHVs were successfully implanted into the orthotopic valve position of a large animal model using a minimally invasive transcatheter (transapical) approach. This study was followed by a similar approach using bone marrow mononuclear cells in a clinically relevant large animal model[16] as well as in the high-pressure environment.[17] The fabrication of autologous cell-based tissue-engineered venous valves (TEVVs) raises significant challenges in the light of the miniaturized dimensions of native venous valves.

Therefore, the present study investigates the principal feasibility of fabricating autologous living (ovine) bone-marrow-derived mesenchymal stem cell–based TEVV substitutes *in vitro*, applicable to minimally invasive (transcatheter) implantation techniques. Moreover, we investigate the macro- and microstructural changes of different cellular compartments of TEVVs during the processes of *in vitro* crimping as well as experimental delivery.

Materials and Methods

Cell harvest and isolation

Ovine mesenchymal stem cells (MSCs) were harvested according to standardized protocols[13,14] from bone marrow aspirates of adult Swiss Alpine sheep. For this purpose bone marrow was harvested from sheep under general anesthesia into a heparinized syringe ($n=3$). All procedures were performed following ethical permission by the cantonal veterinary commission [CVO-137-2009]. In brief, the mononuclear cell (MC) fraction was isolated using a Histopaque® 10771-density gradient (Sigma Chemical Co.). For this purpose the heparinized bone marrow aspirate was layered onto the Histo-paque® and filled up with phosphate-buffered saline (PBS, Sigma). After 30 min of centrifugation the MCs were isolated and washed with PBS. After isolation, MCs were cultured in α-MEM (Ref. 22561; Gibco, Life Technologies). All media were supplemented with 10% fetal bovine serum (Invitrogen Corp.), 1% pen/strep (100 U/mL penicillin, 100 μg/mL streptomycin; Sigma Chemical Co.), 1% Amphotericin B (25 ng/mL Amphotericin B; Sigma Chemical Co.), and 1% Glutamax (Gibco, Inc.). After 48 h of *in vitro* culture the nonadherent cell fraction was removed and the cells were expanded up to passage 6 for seeding onto the composite polymer scaffolds.

Phenotyping of cells

Isolated cells were characterized using immunoflourescence staining. Primary antibodies used for characterization of mesenchymal stem cells were against CD29 (anti-ovine CD29; A. Zannetino), Stro4 (anti-ovine STRO-4; A. Zannetino), CD44 (Santa Cruz, Inc.), CD166 (BioLegend), and CD31 (anti-ovine; BioLegend). Endothelial cells (ECs) were characterized using an antibody against vWF (anti-human; Abcam). Alexa 546 phalloidin (Invitrogen, Inc.) and DAPI (Sigma-Aldrich) were used as control staining. Primary antibodies were detected with Cyanine-2 goat-anti-mouse secondary antibodies (Jackson Immunoresearch Laboratories, Inc.).

For immunofluorescence stainings cells were first washed with PBS and then fixed with 4% paraformaldehyde in PBS for 10 min. Following a second washing phase (PBS), cells were permeabilized in 0.2% Triton X-100/PBS for 10 min and washed again three times in PBS. After blocking with 5% goat serum and 1% bovine serum albumin in PBS for 30 min, primary antibodies were added and incubated for 1 h at room temperature. After three washing steps with PBS, secondary antibodies were added for 45 min at room temperature. The specimens were washed again three times in PBS for 5 min and mounted in commercially available embedding medium (Aqua-Polymount, Polysciences, Inc.). In addition, immunohistochemistry was performed using the Ventana Benchmark automated staining system (Ventana Medical Systems) and antibodies for alpha smooth muscle actin (α-SMA, clone 1A4; Sigma-Aldrich), Desmin (clone D33; DakoCytomatation), Vimentin (mM-anti-human Vimentin; clone Vim 3B4), and vWF (Dako, Inc.). Analysis of the stained sections and cells was carried out using an inverted fluorescence microscope equipped with a CCD camera (ZEISS Axiovert 40 CFL and ZEISS Axioplan II; Carl Zeiss AG). Image processing was performed using the Microsoft Office Picture Manager (Microsoft™).

Flow cytometric analysis

For the purpose of flow cytometry analyses, the *in vitro*-cultured ovine bone-marrow-derived MSCs (BM-MSCs) were harvested from the culture plates using Accutase (Gibco®, Life Technologies) and washed with PBS. Then,

the cells were fixed in 2% paraformaldehyde (P6148; Sigma-Aldrich) for 20 min and washed in PBS. The cells were subsequently permeabilized in BD Perm Buffer III (558050; BD Biosciences) on ice for 30 min and then washed in PBS supplemented with 2% fetal calf serum (FCS). The cells were then incubated with primary antibodies for 45 min on ice, washed twice, and incubated with the secondary antibody for another 45 min on ice. Following washing, the cells were resuspended in PBS + 2% FCS and analyzed using BD FACSCanto II flow cytometry analyzer (Beckton-Disckinson). The antibodies used were the following: Stro-4 (anti-ovine STRO-4; A. Zannettino), CD44 (anti-human Santa Cruz, Inc.), CD166 (BioLegend), CD31 (Dako), IgG1 (BioLegend), and Cy2 secondary antibody anti-mouse (Jackson Immunoresearch Laboratories, Inc.). Acquired flow cytometry data were analyzed and processed using FlowJo software (TreeStar, Inc.).

Scaffold fabrication

Diminutive bi- or trileaflet venous valve scaffolds ($n = 24$) were fabricated from nonwoven polyglycolic acid (PGA) meshes as previously described[15,16] (thickness 1.0 mm; specific gravity 70 mg/cm^3; Cellon) and coated with 1.75% poly-4-hydroxybutyrate (P4HB; TEPHA, Inc.) by dipping into a tetrahydrofuran solution (Sigma Aldrich, Inc.). After solvent evaporation, physical bonding of adjacent fibers and continuous coating was achieved. P4HB is a biologically derived, rapidly degradable polymer, which besides being strong and pliable is thermoplastic (61°C) and can be molded into three-dimensional shapes. The scaffolds were integrated into radially self-expandable nitinol stents (length = 10.0 mm; OD = 12.0 mm when fully expanded at 37°C; OptiMed) by attaching the scaffold matrix to the inner surface of the nitinol stent wires using single interrupted sutures (Polypropylene; Ethicon). After vacuum drying for 24 h, the scaffolds were sterilized using two different protocols: (1) by using ethylene oxide (EtO) gas sterilization (the EtO was allowed to evaporate for 4 days to prevent cytotoxicity.), or (2) by dipping the valves into a 70% ethanol solution for 2 h followed by an overnight exposure to UV light. Next the scaffolds were preincubated in α-MEM (Gibco, Life Technologies) with supplements for 12–24 h to facilitate cell attachment.

Cell seeding

Ovine MSCs were seeded onto diminutive bi- or trileaflet-shaped PGA-P4HB composite scaffolds using different cell seeding numbers (groups: $\sim 1.5/3.0/4.5/5.0/7.0 \times 10^6$ cells/cm^2; $n = 27$) using fibrin as a cell carrier (Sigma Chemical Co.). Fibrinogen (10 mg/mL of active protein) and thrombin were prepared depending on the seeding protocol used and titrated to an optimal clotting time of ~ 30 s by adapting the concentration of fibrinogen. The fibrinogen-thrombin seeding procedure was performed using two different techniques: (1) by seeding cells resuspended in the thrombin solution and subsequent sealing using fibrinogen ($n = 11$ patches, thrombin concentration: 115.7 IU/mL) as previously published,[18] or (2) by seeding the cells resuspended in a fibrinogen-thrombin cosolution ($n = 15$ patches, thrombin concentration: 10 IU/mL) as previously described.[19] After static incubation of seeded constructs in α-MEM (Sigma Chemical Co.; 10% fetal bovine serum [FBS]; pen/strep and Amphotericin-B supplement) for short periods (1, 4, or 7 days), they were placed into an inverted-flow bioreactor system with diastolic (flow) pulse stimulation mimicking the native cardiovascular environment. For dynamic conditioning the medium was supplemented with 0.9 mM of L-ascorbic acid-2-phosphate (Sigma Chemicals, Inc.). The pulsatile flow was slightly increased over the study period (from 1.5 mL/min flow to 3 mL/min flow) and α-MEM was exchanged every 3–4 days. The constructs were harvested after 1–2 or 11–14 days of dynamic conditioning. After harvesting from the bioreactor, the constructs were (1) endothelialized ($n = 11$; see the ''Endothelialization and crimping analysis'' section) followed by further static conditioning in EGM-2™ (Lonza) medium, and (2) exposed to a crimping procedure ($n = 18$) or analyzed immediately.

Endothelialization and crimping analysis

ECs were isolated according to previously published protocols.[14] Briefly, the ovine blood vessels were flashed with PBS and incubated for 30 min in collagenase (2 mg/mL, Collagenase A; Roche Diagnostics GmbH). After incubation, the cell suspension was flushed out with EBM-2 medium (EBMTM; Lonza, Inc.), and cultured on six-well plates until confluency and expanded. The medium was supplemented with 2% FBS, vascular endothelial growth factor, human fibroblast growth factor, human recombinant long-insulin-like growth factor-1, human epidermal growth factor, gentamycin and amphotericin (GA-1000), hydrocortisone, heparin, and ascorbic acid. For endothelialization, TEVV leaflets were seeded with $0.6–1.3 \times 10^6$ cryopreserved ovine ECs per cm^2. The constructs were cultured for 48 h in endothelial medium (EGM™ -2; Lonza Group AG; Medium B constructs) to ensure adequate attachment of the cells. Prior to seeding, ovine ECs were labeled using carboxyfluorescein-diacetate-succinimidyl-ester at a concentration of 25 μM according to the manufacturers' instructions (CFSE, CellTrace™; CFSE Cell Proliferation Kit, C34554; Invitrogen Corp.). After static incubation the constructs were crimped for ~ 10 min ($n = 15$ leaflets) to a size of 16 F (~ 5 mm) using a customized crimping machine (Edwards LifeSciences, Inc.). Using the IVIS Imaging System (PerkinElmer Life Sciences, Inc.), CFSE-labeled ovine EC-seeded TEVVs were scanned before and after crimping and the changes of fluorescence (counts) were determined. For detection of CFSE-labeled ECs pre- and postcrimping (CellTrace™, CFSE Cell Proliferation Kit, C34554; Invitrogen Corp.) a band-pass filter from 445 to 490 nm and a long-pass filter over 515 nm for excitation and emission light, respectively, were used. The fluorescence was detected by a CCD camera. The data were analyzed using the Living Image® software (Living Image® 3.2; PerkinElmer Life Sciences, Inc.). For assessment of the location and density of seeded ECs on the surface, the constructs were scanned using a StereoLumar.V12 stereomicroscope (Carl Zeiss).

Qualitative tissue analysis

The tissue composition of TEVV constructs was analyzed qualitatively using immunohistochemistry and/or histology and compared with native ovine venous valve leaflets

(jugular vein and saphenous vein valve leaflets). The tissue sections were studied using hematoxylin and eosin (H&E) and Masson–Trichrome stainings. In addition, immunohistochemistry was performed using the Ventana Benchmark automated staining system (Ventana Medical Systems) and antibodies for α-SMA (clone 1A4; Sigma-Aldrich), Desmin (clone D33; DakoCytomatation), and Vimentin (clone VIM3B4; DakoCytomatation). All sections were analyzed using an inverted light/fluorescence microscope and compared to native tissues (ZEISS Axiovert 40 CFL and ZEISS Axioplan II; Carl Zeiss AG).

Quantitative explant tissue analysis

TEVV constructs ($n = 14$ representative samples) were minced, lyophilized, and analyzed using biochemical assays for total DNA content as an indicator for cell number, hydroxyproline (HYP) content as an indicator for collagen, as well as for glycosamnioglycan (GAG) content. For measuring the cellularity of the constructs, the DNA amount was quantitated according to an established protocol.[20] Briefly, papain-digested samples were incubated with Hoechst dye at final concentration of 2.5 nM (Bisbenzimide H 33258; Fluka) for 10 min at room temperature protected from light. Resulting fluorescence was quantified and compared to standards made of calf thymus DNA (Sigma Chemical Co.) with a fluorometer (Fluostar; BMG, 355 nm excitation/460 nm emission). The GAG content was determined using a modified version of the protocol described by Farndale *et al.*[21] and a standard curve was prepared from chondroitin sulfate from shark cartilage (Sigma Chemical Co.) in addition to the samples. Briefly, the GAG amount was determined colorimetrically using di-methyl-methylene blue stain [DMMB: 46 μM 1,9-di-methyl-methylene blue, 40.5 mM Glycin, and 40.5 mM NaCl (pH 3)], following complete papain digestion of the constructs in digestion buffer [100 mM sodium phosphate (pH 6.5), 5 mM L-cysteine, 5 mM EDTA, and 125 mg/mL papain (Sigma)] in a 4:15 ratio of sample:DMMB. The absorbance was measured at 540 and 595 nm; the values obtained at 595 nm were subtracted to the ones of 540 nm.

The amount of collagen (HYP) was determined with a modified version of the protocol provided by Huszar *et al.*[22] Briefly, minced tissue samples were hydrolyzed in NaOH (Fluka) at a final concentration of 4 mM in an autoclave at a temperature of 120°C for 10 min. The solution was neutralized by adding an equal volume of 1.4 M citric acid (Fluka). Chloramin-T was added to a final concentration of 56 mM and the samples were oxidized for 20 min before adding aldehyde/perchloric acid solution at a final concentration of 0.5 M. The chromophore was allowed to develop at 65°C for 15 min. The absorbance of the obtained solutions was determined at 550 nm. The amount of HYP present in the hydrolysates was determined from a standard curve using known amounts of trans-4-hydroxy-L-proline (Sigma Chemical Co.).

Grating interferometry

PGA-P4HB starter matrices as well as bioengineered constructs—in crimped as well as uncrimped state—were evaluated using grating interferometry (GI; $n = 3$). GI represents a hard X-ray imaging method that simultaneously exploits absorption as well as phase information, the latter typically providing superior contrast if applied to soft-tissue samples.[23–25] Experiments were performed at the TOmographic Microscopy and Coherent rAdiology experimenTs (TOMCAT) beamline of the Swiss Light Source (Villigen).[26] Optimal sensitivity toward density variations was ensured by choosing a photon energy of 25 keV and an intergrating distance of 121 mm.[27] Samples were embedded in 2% agarose gel within an Ependorff cylinder for mechanical fixation. Tomography scans were performed with 1081 projections over 180° and five-phase steps. Total scan time was ~1 h. Tomographically reconstructed multislice information was combined in three-dimensional images and different stages of sample development were compared.

Scanning electron microscopy

Representative samples of the TEVV leaflet and conduit areas of all (crimped and uncrimped) groups were fixed in 2% glutaraldehyde for >24 h. After preparation, samples were sputtered with gold and investigated using a Zeiss Supra 50 VP Microscope (Zeiss).

Simulated delivery and crimping analysis

For evaluation of the effect of the delivery procedure on the structural integrity of the mesenchymal stem cell–based bioengineered venous valves, the constructs were crimped using a commercially available crimping machine ($n = 19$; Edwards LifeSciences, Inc.). For crimping of MSC-based or endothelialized constructs the radial diameter of the stent was reduced from 12.0 mm down to ~5.0 mm (16 F) before being introduced into the catheter system with a final diameter of 8.0 mm prior to deployment. The constructs were crimped for 7 min (mesenchymal stem cell group) or 10 min (EC group) and then deployed by pushing the valves out of the sheath system ($n = 7$; see Fig. 2e–f).

Statistical analysis

The results on the quantification of ECs are presented as mean ± standard deviation. For the statistical comparison of crimped versus non-crimped TEVV samples [IVIS® analysis and extracellular matrix (ECM) analyses] an unpaired *T*-test was performed (SPSS 17.0; IBM). For comparing the percental cellular loss with each group (signal loss per leaflet) a paired *T*-test was performed (SPSS 17.0; IBM). Biochemical measurements are presented as mean ± standard error of the mean. A p-value < 0.05 was considered statistically significant (SPSS 17.0; IBM and Microsoft Office Excel 2007; Microsoft, Inc.).

Results

Morphology and phenotype of ovine bone marrow–derived mesenchymal stem cells

Outgrowing ovine BM-MSCs (oMSCs) expressed myogenic markers, such as α-SMA and vimentin (Fig. 1c–e). Desmin—another common smooth muscle cell marker—was not expressed in expanded oMSCs (Fig. 1f). In immunohistochemistry oMSCs revealed expression of several ovine (mesenchymal) stem cell markers, such as CD29 or CD44, STRO-4, and CD166, while no positive signal was

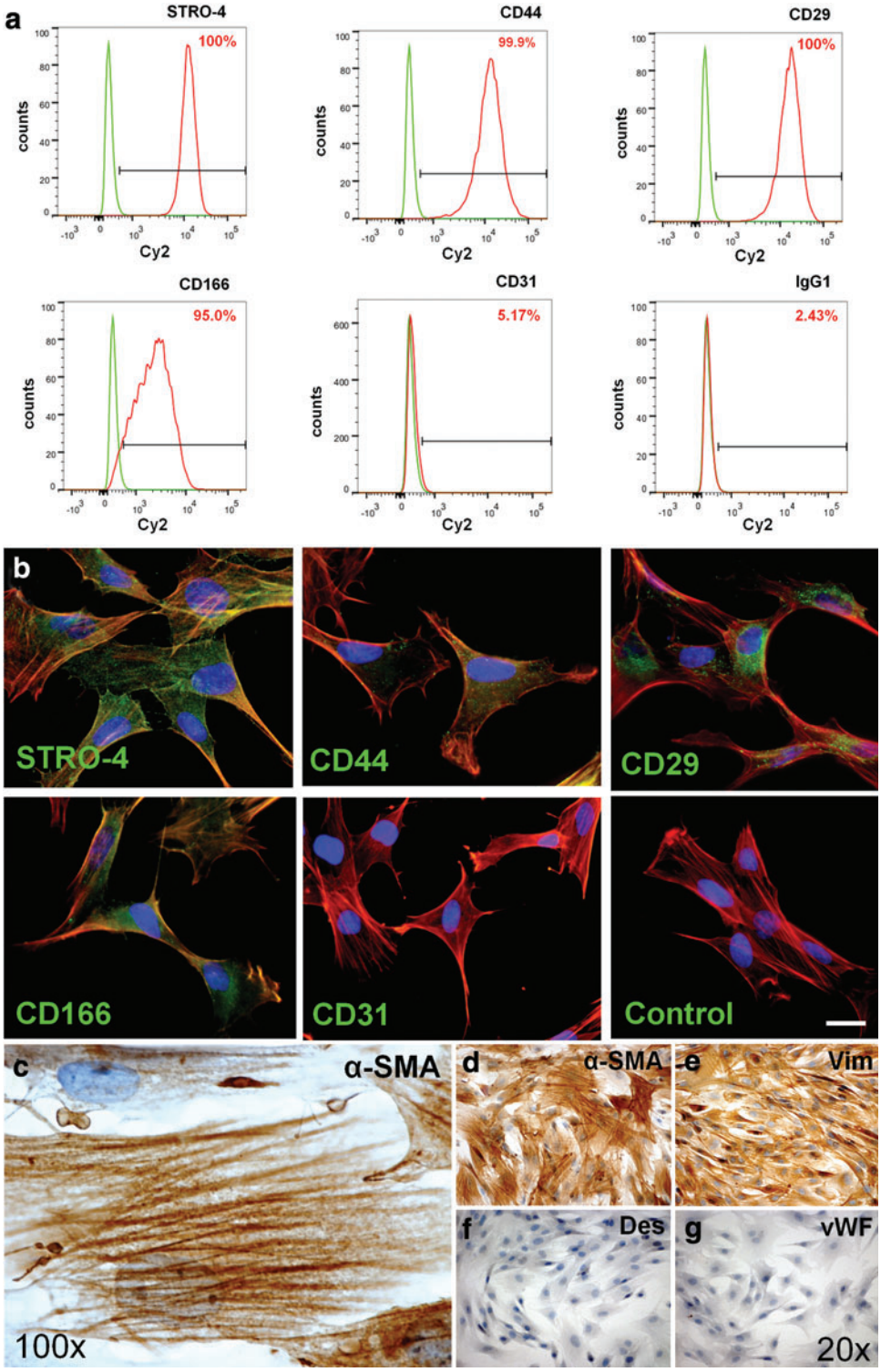

FIG. 1. Immunohistochemical phenotype of ovine bone marrow–derived mesenchymal stem cells (oMSCs). Isolated adherent ovine MSCs show positive signals for CD166, CD44, CD29, and STRO-4 in flow-cytometry analysis **(a)**. No signal was detected for CD31 **(a;** IgG1 served as isotype control). In immunohistochemistry **(b–g)**, oMSCs show expression of myogenic markers **(c–e)**, including alpha-smooth muscle actin (α-SMA) **(c, d)** and vimentin **(e)**. Also stainings for common ovine stem cell markers **(b)**, including CD29, CD166, STRO-4, and CD44, are positive **(b;** scale bar = 16 μm). No positive signal was found for CD31 **(b)**, IgG1-isotype control, Desmin **(f)**, and von Willebrand factor (vWF) **(g)**. Color images available online at www.liebertpub.com/tec

found for vWF, CD31, and isotype controls (Fig. 1b, g). Flow cytometric analysis revealed high expression levels for CD29, CD166, CD44, and also STRO-4; however, no expression of CD31 could be detected in oMSCs (Fig. 1a).

Analysis of TEVVs: macroscopic appearance

After successful isolation, oMSCs were expanded and seeded onto PGA-P4HB composite scaffolds for static (up to 7 days) and dynamic conditioning (up to 14 days). Static control constructs were cultured under nondynamic environment for up to 3 weeks and harvested accordingly ($n = 41$). The bi- and trileaflet-valve-shaped constructs were intact, pliable, and mobile (Fig. 2a–f) after dynamic (pulsatile) conditioning in a bioreactor system with neotissue densely covering the bioengineered valves independent of the conditioning protocol used. After harvest, the fused bi- and trileaflet structures (Fig. 2a–c, f) were successfully

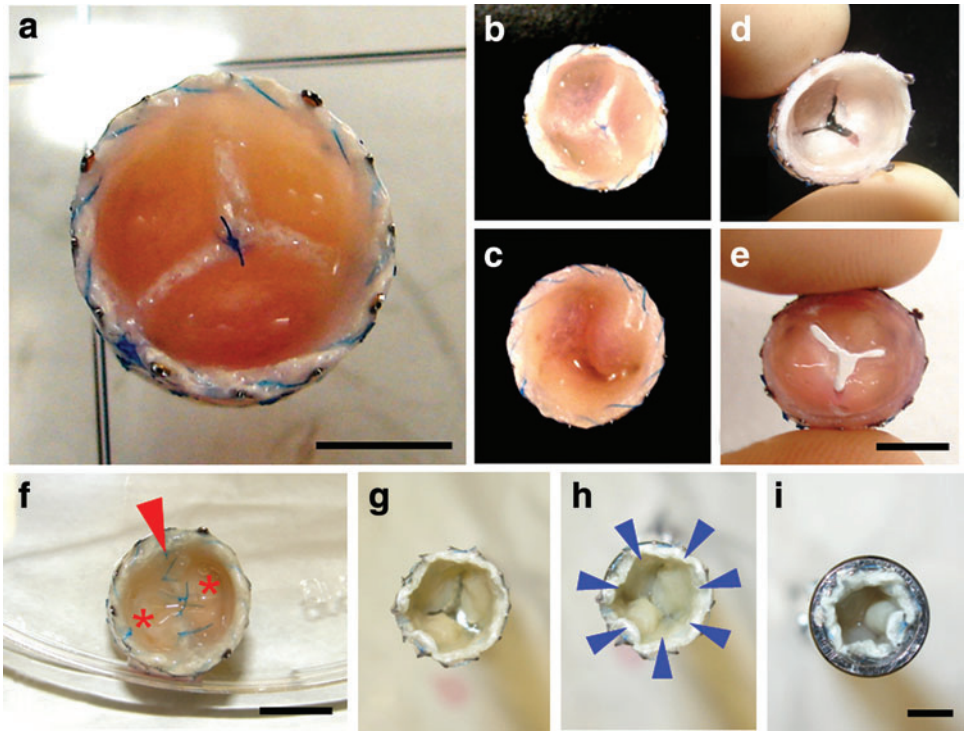

FIG. 2. Macroscopy of tissue-engineered bi- and tricuspid venous valves. Tricuspid **(a–e)** and bicuspid **(f)** tissue-engineered venous valves (TEVVs) were fabricated using a diastolic (flow) pulse duplicator system **(a–f:** scale bar = 5 mm**)**. After harvest, the fused leaflets **(a–c, f; c:** inferior view; **f**, arrow = value opening**)** were separated **(d, e)** and a series of valves was crimped and inserted into a delivery device **(g–i:** scale bar = 4 mm; **h:** arrow = crimping forces; asterisk = leaflets**)**. Color images available online at www.liebertpub.com/tec

separated from each other (Fig. 1d, e) using a scalpel without laceration of the constructs. Separated TEVV constructs were then successfully used for crimping and/or simulated delivery analysis (Fig. 2g–i).

Qualitative tissue analysis: histology and immunohistochemistry

Tissue-engineered constructs grown under static conditions (control constructs; $n = 41$) demonstrated cellular ingrowth but little tissue formation and production of ECM in Trichrome-Masson staining (Fig. 3k, l). In contrast, constructs of all (long term) dynamic groups (7/14 days) showed layered tissue arrangement in H&E staining (Fig. 3a, b) and substantial tissue formation with production of ECM in the conduit wall (Fig. 3c, d) as well as in the TEVV leaflet structures (Fig. 3e, f). In detail, Trichrome-Masson staining highlighted collagen formation at the outer (luminal) layers of TEVVs (Fig. 3c, α), whereas in the center, loosely arranged ECM with scaffold remnants was detectable (Fig. 3c, β; arrows in Fig. 3c, d represent residual scaffold fibers). α-SMA-positive cells were present in superficial layers of both, static and dynamic, constructs (Fig. 3g–h).

Crimping analysis: ECM

For quantitative assessment of the ECM components, biochemical assays for the determination of the DNA, GAG, and HYP were performed for different cultivation time points and crimping stages. Following *in vitro* conditioning, all groups—independent of the crimping stage—showed GAG values comparable to native. When comparing GAG values of crimped versus uncrimped samples, no significant differences were found ($p > 0.05$; see Fig. 4a). Also the cellularity did not differ significantly between crimped and uncrimped samples ($p > 0.05$; see Fig. 4b). For HYP the values were substantially lower than the native control and also showed no significant differences between crimped and uncrimped tissues ($p > 0.05$; see Fig. 4c).

Crimping analysis: macroscopy and histology after simulated delivery

TEVVs ($n = 18$) were crimped using a commercially available crimping device, introduced into a delivery system ($n = 7$), and deployed (experimental delivery). Histological analysis after crimping and simulated delivery included comparison after crimped ($n = 18$) versus uncrimped ($n = 9$) TEVVs (Fig. 5b–f). Trichrome-Masson staining revealed integrity of the α-SMA-positive luminal collagen layer after crimping and simulated delivery. No signs for impairment of the construct integrity on the histological level—such as holes, fissures, or fractures—could be identified. However, this assessment is significantly limited as to the two-dimensional character of the analysis. Also, macroscopically no signs of impairment or inhomogeneity could be identified. However, on the macroscopic level, the aspect of lower coadaptation of the leaflets (radial leaflet length shortening) was observed when compared to the precrimping state.

Crimping analysis: scanning electron microscopy

After crimping (and simulated delivery) of (non-endothelialized) TEVVs, surfaces were analyzed using scanning electron microscopy (SEM). In SEM the cells revealed homogenous orientation in several regions (Fig. 6a–j); however, no consistent cell arrangement was observed through the entire constructs as to the complex diastolic valvular flow profile of this (flow pulse duplicator) bioreactor system. Similar to histology, also SEM revealed no structural impairment, such as cracks or holes, on the crimped

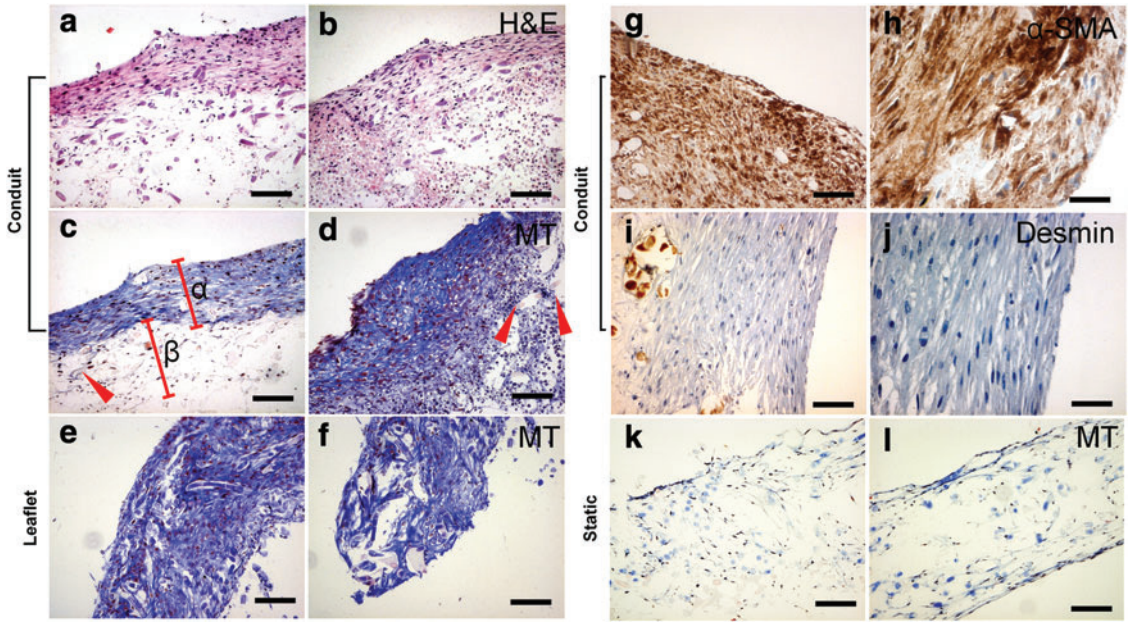

FIG. 3. Histological analysis of TEVVs. Dynamic TEVV constructs showed layered tissue arrangement in hematoxylin and eosin (H&E) staining **(a, b)** with surface-mediated collagen formation visible in Masson-Trichrome staining in the conduit wall **(c, d;** collagen matrix: α; subcollagen nondegraded scaffold zones: arrow and β) and the leaflet **(e, f)**. In the wall area, also α-SMA-positive regions were found **(g–h)** with no positivity for Desmin **(i, j)**. In static (nondynamic control) constructs only a small band of cells (close to the surface) could be identified **(k, l)**. **(a–f, k, l**: 10× magnification, scale bar ~100 μm; **g, i:** 20×, scale bar ~50 μm; **h, j:** 40×, scale bar ~25 μm). Color images available online at www.liebertpub.com/tec

(Fig. 6f–j) versus the uncrimped construct surfaces (Fig. 6a–e). However, in some regions of the crimped constructs, "bare" PGA fibers (not covered with cells) could be identified (Fig. 6h; arrows), whereas in the matching uncrimped controls, PGA fibers were densely covered by seeded oMSCs (Fig. 6e; arrows). However, given the limited number of samples, these qualitative findings require further confirmation and quantitative assessment in future experiments. Besides this aspect, no changes on the cellular level on the construct surfaces could be identified in SEM.

Grating interferometry

For three-dimensional analysis of *in vitro* tissue formation and degradation of the composite starter matrix and—importantly—for the assessment of three-dimensional crimping effects, a series of three constructs was investigated using GI. GI samples comprised unconditioned (unseeded) PGA-P4HB starter matrices, and TEVVs in crimped and uncrimped states. In comparison to the unconditioned scaffold constructs (Fig. 7a–d), the conditioned TEVV samples (Fig. 7e–l) revealed clear tissue formation embedded into remnants of the PGA-P4HB scaffold meshwork. The signal for the composite scaffold was reduced after 14 days of dynamic conditioning (Fig. 7e–h), suggesting degradation of the composite starter matrix components as confirmed by histology (Fig. 3a–f). As previously reported,[19] in the three-dimensional GI reconstruction, the degradation was inhomogeneous with zones of higher versus lower degradation (Fig. 7f, h: blue lines indicate zones of higher degradation). This suggests a cluster-like (inhomogeneous) tissue maturation within the bioengineered TEVVs. The crimped bioengineered construct showed a similar inhomogeneous, cluster-like matrix composite degradation. Using a manual segmentation approach (representative segmented slices are shown in Fig. 7g–k) the proportions of scaffold versus biological matrix were quantified revealing that the proportion of biological matrix did not undergo substantial volumetric changes during the crimping procedure (matrix ratio at precrimping state: 76% ± 6% versus matrix ratio at postcrimping state: 83% ± 2%). In spite of the lack of clear changes regarding

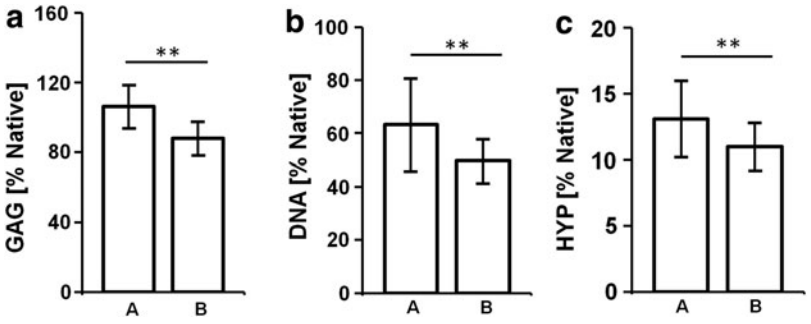

FIG. 4. Biochemical extracellular matrix (ECM) analysis. Analysis for ECM components revealed no significant differences for glycosaminoglycans (GAG; **a**), DNA **(b)**, and hydroxyprolines (HYP; **c)** when comparing uncrimped (A) versus crimped (B) constructs (values: % of native control; mean ± SEM; ** = $p < 0.05$).

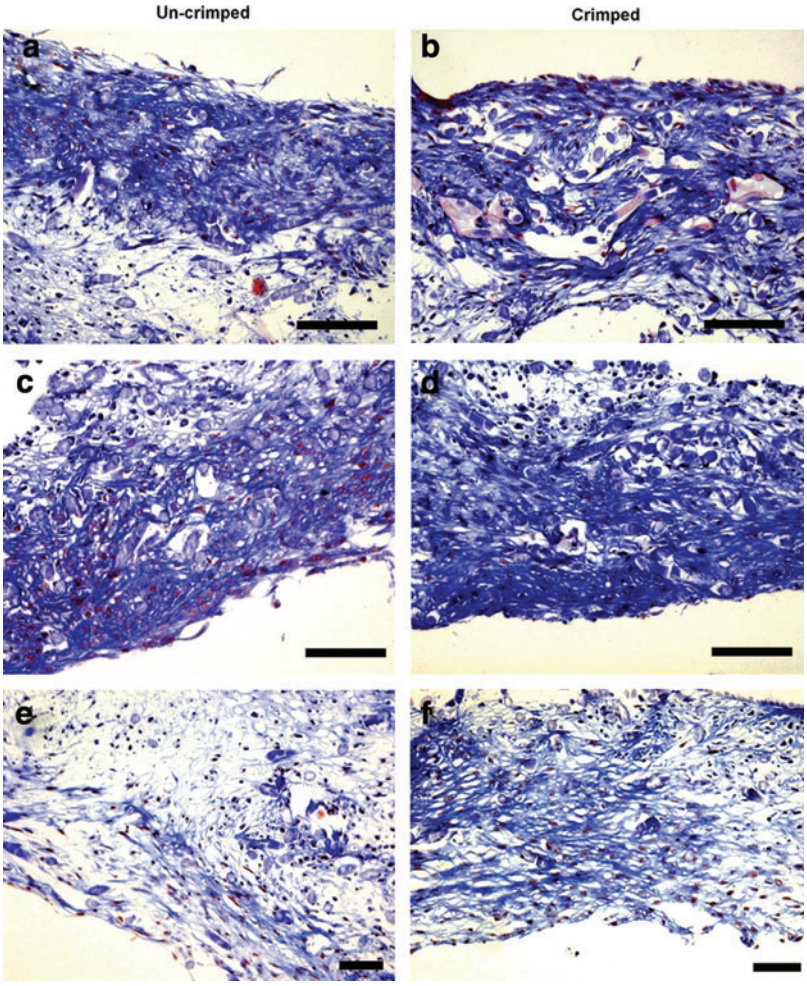

FIG. 5. Histological analysis of crimped versus uncrimped TEVV constructs. The histological analysis of three individual bioengineered venous valves before **(a, c, e)** and after **(b, d, f)** crimping (Masson Trichrome) showed layered tissue formation with collagen-rich elements close to the surface of the bioengineered constructs in both groups **(a–f)**. In the group of crimped samples no signs of surface laceration, cracks, holes, or other signs of structural impairment could be identified on the histological level **(b, d, f)** (scale bar = 100 μm). Color images available online at www.liebertpub.com/tec

the ECM portions of the bioengineered matrix, the distribution of the matrix was less homogeneous when compared with the precrimping state (see Fig. 7h, l; red and blue lines). These changes in the matrix could be due to the tissue compaction effects throughout the crimping procedure or represent artifacts of the inhomogeneous degradation behavior. However, given the complexity of the analysis and the low sample number, this finding needs further evaluation by future experimental studies.

Crimping analysis using planar fluorescence reflectance scanning

As part of the conventional *in vitro* tissue engineering approach, MSC-based matrices are endothelialized prior to *in vivo* implantation. However, in case of minimally invasive delivery, the crimping may impair the integrity of the vulnerable EC coverage on the TEVV surface. For assessment of the loss of ECs a representative series of bicuspid ($n = 6$) as well as tricuspid TEVV leaflets ($n = 15$) was seeded with cryopreserved ovine CFSE-labeled ECs (see Fig. 8a–d). After static *in vitro* incubation the valves were crimped using a clinically relevant protocol (10 min, ~16 F) and the loss of CFSE signal was quantified using a planar fluorescence reflectance CCD camera. As shown in Figure 8 the CSFE signal per leaflet (Fig. 8e) was reduced significantly [reduction for protocol (1) 73.8% ± 25.9% and for protocol (2) 51.49% ± 19.8%; Fig. 8f; all p's < 0.001] during the crimping procedure, while unseeded leaflets showed no significant reduction of the fluorescence in the leaflets (reduction of 10.5% ± 13.6%; Fig. 8f; $p > 0.05$). These results suggest that there is a significant loss of ECs during the crimping procedure of TEVVs. However, interestingly the cellular loss was significantly different between the different static incubation protocols (1) and (2) ($p < 0.001$), suggesting further that longer static incubation prevents cellular loss of ECs during crimping (Fig. 8d).

Discussion

CVI is a common pathology of the cardiovascular system and represents a global health problem.[5] In the United States 10–35% of the adult population is affected and these numbers are expected to increase in the future given the demographic development.[7,28] CVI is caused by an incompetence of the venous valves, which causes retrograde venous flow (reflux) with distal venous hypertension and a plethora of further sequela.[29] Treatment of CVI is dominated by nonsurgical modalities, which are mainly of palliative nature and are deemed ineffective of changing the underlying cause of the disease. Therefore, several surgical and—in the recent years—interventional experimental approaches have focused on the replacement of the diseased valvular structures using prosthetic venous valves. Since the

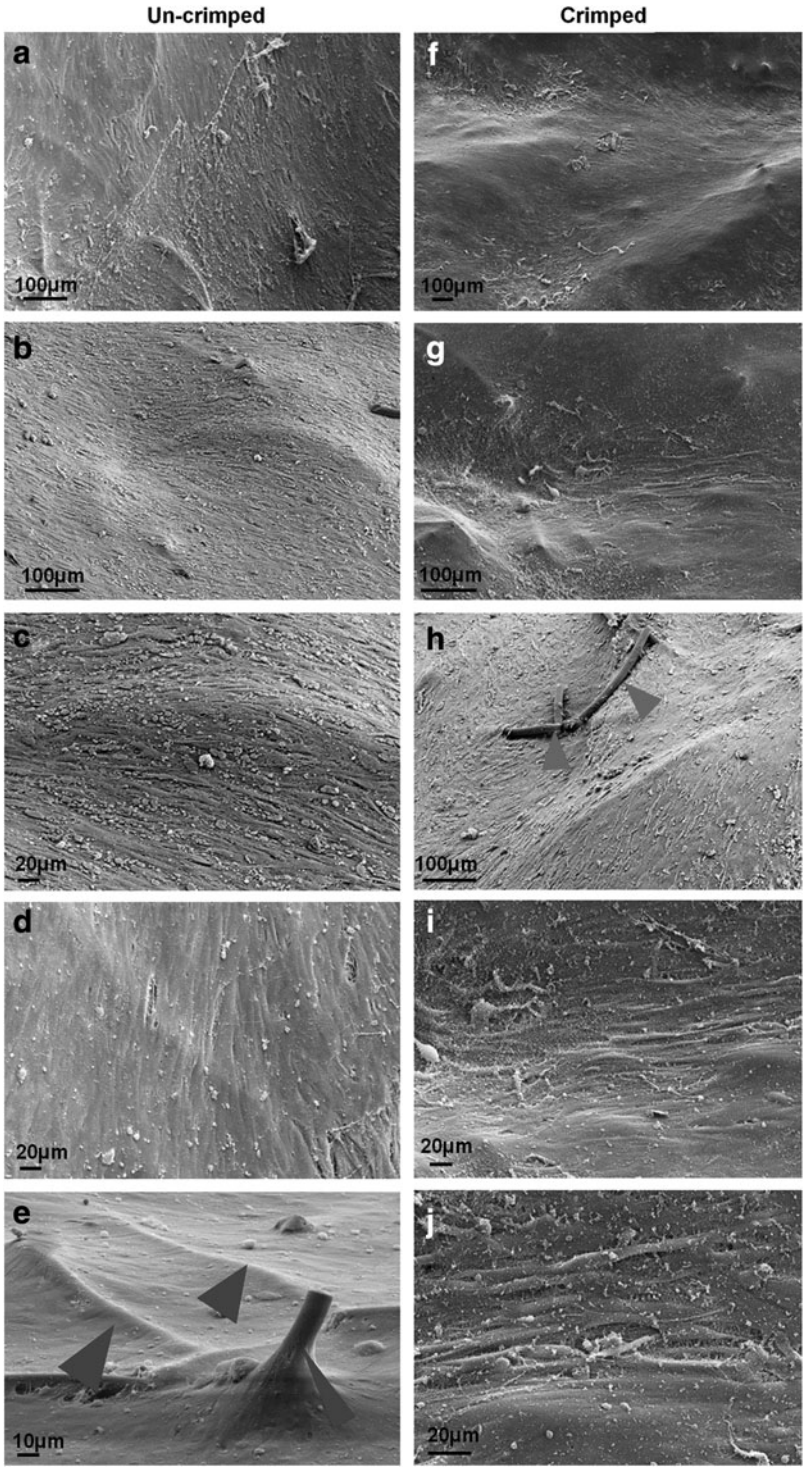

FIG. 6. Scanning electron microscopy (SEM) analysis of crimped versus uncrimped TEVV constructs. SEM analysis of uncrimped samples revealed confluent coverage of the bioengineered constructs by oMSCs **(a–d)** with cells densely covering polyglycolic acid (PGA) fiber components **(e;** arrows = PGA fibers**)**. This confluent cellular coverage of the surface remained unchanged throughout the crimping procedure **(f, g, i, j)**; only in some areas uncovering of PGA fiber elements was observed **(h;** arrows**)** not evident in the uncrimped samples **(e;** arrows**)**.

mid-60s several different valve prostheses have been investigated on the experimental and clinical level involving single-, double-, or trileaflet designs, and involving allogenic, xenogenic, or synthetic materials.[7,30,31] Initial clinical attempts that focus on cryopreserved homografts showed poor clinical outcomes with rejection of the transplanted valves, leading to high morbidity and occlusion rates.[32] This stimulated the development of autologous transplantation strategies in order to prevent graft rejection complications. Although some of these approaches showed promising experimental[33,34] and clinical results,[35,36] several approaches were limited by the lack of adequate or sufficient amounts of autologous replacement structures.[7]

Cardiovascular tissue engineering could overcome these limitations by providing autologous cell-based replacement structures with absence of immunogenic rejection.[8,9] The concept of cardiovascular tissue engineering is based on biodegradable scaffold materials that are seeded with autologous cells and cultured under native-like flow conditions *in vitro* to generate native-analogous tissue-engineered

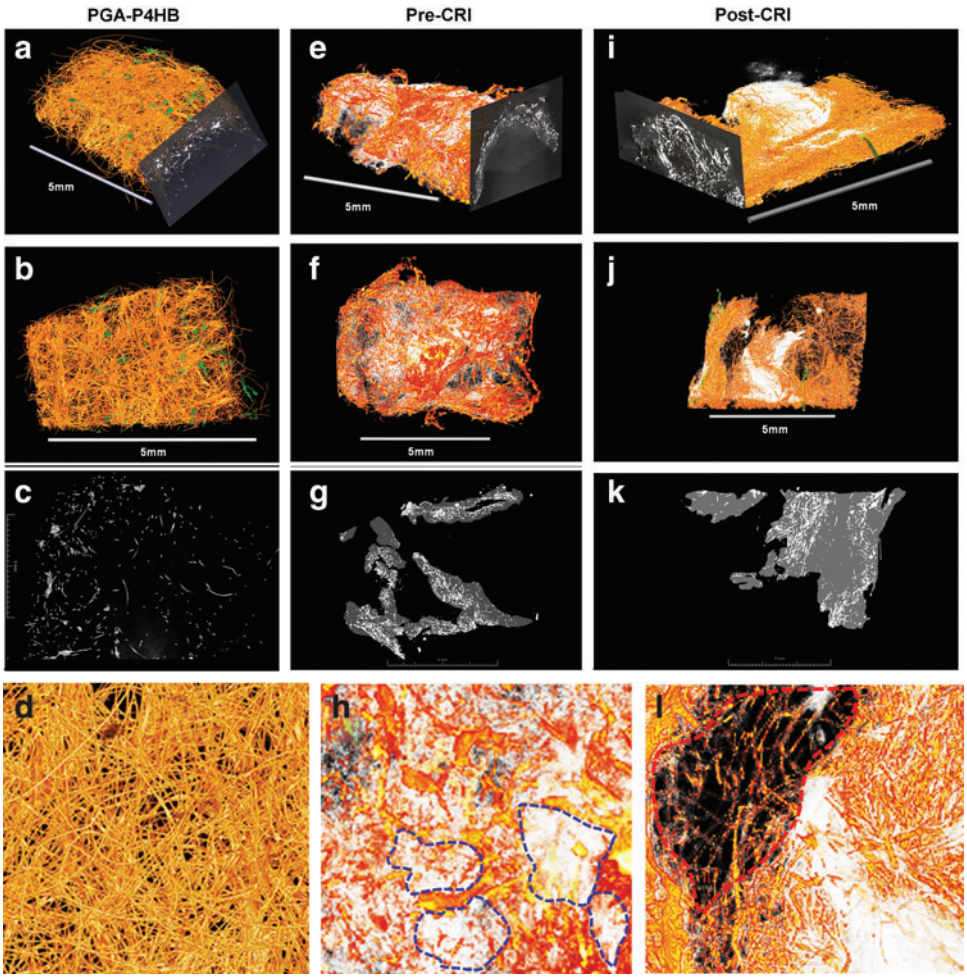

FIG. 7. Grating interferometry (GI) of TEVV constructs. GI analysis of PGA–poly-4-hydroxybutyrate (P4HB) starter matrices showed homogeneous scaffold networks **(a–d**; unconditioned bare scaffold material**)**. After dynamic *in vitro* conditioning **(**conditioned samples: **e–l)** inhomogeneous degradation of the scaffold matrix was observed (blue lines indicate major degradation zones; **e–h)**. After crimping of the construct, the aspect of ''shifting'' of the ECM components could be observed with areas of biological matrix accumulation and areas with less matrix present **(i–l**; red line: area without substantial neomatrix present). [Pre-CRI = before crimping; Post-CRI = after crimping]. Color images available online at www.liebertpub.com/tec

constructs.[9] In particular in the field of heart valve regeneration, several recent preclinical large animal trials involving sheep[14,15,17] and non-human primate models[16] showed promising initial results and underline the potential of this technology for future therapeutic concepts.

Given the major complications when using xeno- or homogenic venous valve transplants, Teebken *et al.*[37] investigated for the first time TEVVs based on a homologous decellularized matrix in the ovine model. After removal of cellular elements, the valves were repopulated with autologous myofibroblasts and implanted into the external jugular veins with patency up to 12 weeks. In spite of promising short-term results, also in these homologous reseeded constructs, immunologic rejection phenomena were observed with inflammation and neointima formation being evident in the TEVV explants.[37] In addition, the widespread issue of scarcity of human donor organs available for transplantation[38] severely limits a widespread application of concepts based on healthy human homologous transplants for treatment of such frequent pathologies.

Therefore, the present study investigates for the first time the fabrication of BM-MSC-derived miniaturized TEVVs based on a synthetic, completely biodegradable PGA-P4HB composite matrix. Given their fully autologous nature, these living patient cell–derived constructs hold the potential to overcome the limitations of immunogenic rejections reported for xenogenic or homogenic transplants and are not dependent on the availability of human healthy donor tissue.

However, in recent years the field of heart valve and also venous valve implantation has encountered a major technological revolution with development of percutaneous low-invasive delivery techniques.[39] In venous valve repair several clinical trials have been initiated using percutaneous transcatheter delivery methods. Borst *et al.* reported clinical phase I and II trials using glutaraldehyde-fixed bovine jugular valve–based venous xenografts integrated into a nitinol stent for transcatheter implantation.[40–42] Also the group of Pavcnik *et al.* reported a minimally invasive transcatheter approach based on a xenogenic bioprosthetic venous valve system with initial promising results.[43–45] Therefore, besides the use of an autologous low-invasive cell source (such as BM-MSCs), a clinically relevant TEVV concept requires a combination of the tissue engineering technology with minimally invasive delivery methods, which has already been successfully demonstrated for heart valve tissue engineering in the ovine model for the low-[14] as well as the high-pressure system[17] up to 2 months *in vivo*. Recently, stented TEHVs could also be minimally invasively delivered into the orthotopic pulmonary position of a clinically relevant non-human primate model that shows promising results *in vivo* with confluent endothelialization and interstitial valve remodeling.[16]

Also in the present study adequate tissue formation was achieved using a diastolic pulse duplicator system with

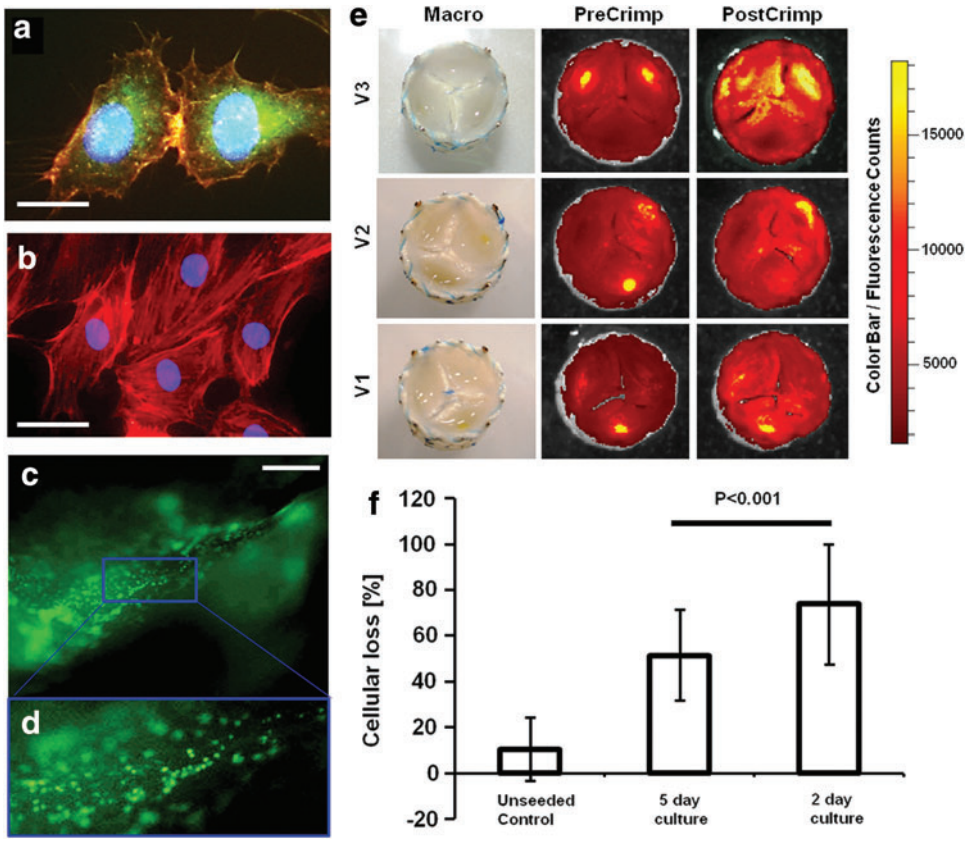

FIG. 8. Planar fluorescence reflectance imaging analysis of crimped TEVV constructs. TEVVs were seeded with CFSE-labeled endothelial cells (ECs) that stained positive for vWF **(a;** green = vWF, blue = DAPI, red = phalloidin; **b** = isotype control). After seeding (stereomicroscopy analysis of the ECs on the leaflet; **c, d**; scale bar = 500 μm) the valves were crimped (for 10 min, ~5 mm) and the fluorescence signal was measured before and after crimping **(e;** V1–V3 show three representative examples**)**. When quantified, the fluorescence in the seeded constructs decreased during the crimping procedure, while the fluorescence signal of unseeded control areas remained unchanged **(f)**. Interestingly, the cellular loss significantly decreased when increased static conditioning periods were used, indicating that adapted protocols may prevent the EC loss **(f)** (scale bars: **a,** 16 μm; **b,** 25 μm). Color images available online at www.liebertpub.com/tec

layered collagen arrangement, increasing glycosaminoglycan content and surface endothelialization. However, as previously reported for bioprosthetic valves,[46] the crimping and minimally invasive delivery procedure may affect the viable tissue components of the bioengineered venous valves. Therefore, representative numbers of BM-MSC-derived crimped and uncrimped TEVV constructs were analyzed using SEM, histology/immunohistochemistry, GI, and biochemical ECM analysis. Neither SEM nor histological analyses revealed lacerations or changes of the TEVV constructs during the crimping procedure, also no compression effects were observed as reported by previous studies that focus on human-cell-based constructs.[19] GI, a novel tool for 3D analysis of tissue-engineered constructs, showed inhomogeneity of the ECM arrangement in the crimped sample; however, these results were limited by the low sample number ($n = 3$) of this pilot analysis and the influence of inhomogenous degradation/tissue formation remains unclear. As reported in a previous study,[19] some minor changes in the biochemical ECM parameters were observed; however, none of those changes were statistically significant. These results suggest that the BM-MSC-derived bioengineered tissue component of the TEVV constructs was not affected by the crimping procedure on the structural level. This finding is supported by previous experiments that focus on tissue-engineered occluder membranes, which also showed no significant changes after crimping on the mesenchymal/fibroblastic cell level. However, in these studies[19] morphological changes were reported for the EC level in scanning ion conductance microscopy. Therefore, in the present study, we endothelialized a series of TEVV samples with CFSE-labeled cryopreserved ovine ECs and measured the cellular loss during the crimping procedure using the IVIS® system. This revealed that crimping (10 min; ~5 mm) did not significantly change the overall DNA amount in the constructs but resulted in a significant loss of ECs (~74% of initially seeded cells) on the surface. This suggests that seeded EC monolayers may represent the ''weakest'' part of bioengineered constructs exposed to crimping procedures. When considering recent experimental results, the relevance of this EC loss seems unclear. First, because implantation of non-endothelialized heart valve constructs into non-human primates resulted in almost confluent endothelialization already after 4 weeks *in vivo*,[16] and second, because novel approaches completely circumvent the endothelial component and focus on the implantation of decellularized and/or

reseeded tissue-engineered constructs for heart valve regeneration.[47] In addition, the loss of ECs during the crimping procedure could be significantly reduced by increasing the static *in vitro* conditioning phase. However, the loss of ECs and the associated thrombogenicity certainly represents a major question to be answered in future preclinical *in vivo* animal trials as the lack of major thrombogenicity displays an indispensable prerequisite for a possible clinical translation of the involved technology.

In conclusion, this feasibility *in vitro* study successfully combines two evolving technologies, that is, cardiovascular *in vitro* tissue engineering as well as minimally invasive valve replacement techniques. The presented data shows that the *in vitro* fabrication of miniaturized living tissue-engineered valves based on autologous (mesenchymal) stem cells and on fully biodegradable (composite) polymer scaffolds integrated into nitinol stent systems is feasible in the ovine model and lays the foundation for an animal *in vivo* trial in the near future. These upcoming *in vivo* experiments will have to carefully assess the leaflet functionality as well as the *in situ* remodeling of the TEVV constructs in order to bring the technology closer to a possible future clinical translation.

Acknowledgments

The current study represents a collaboration. The authors thank Klaus Marquardt (ZMBZ), Andres Kaech (ZMBZ), Pia Fuchs, Burkhardt Seifert (IFSPM), and Ursula Steckholzer. This work was supported by the Swiss National Science Foundation (320030-122273), (IZK0Z3_140187), and (310030-143992); the EMDO Foundation (791-2012); the Swiss Heart Foundation; the Start-up Grant of the Clinical Trials Center/University Hospital Zurich (DFL-1232); the 7th Framework Programme, Life Valve, European Commission (242008); the Centre d'Imagerie BioMedicale (CIBM) of the UNIL, UNIGE, HUG, CHUV, EPFL; and the Leenaards & Jeantet Foundations.

Disclosure Statement

The authors have no potential conflicts of interest to disclose.

References

1. Eberhardt, R.T., and Raffetto, J.D. Chronic venous insufficiency. Circulation **10,** 111, 2005.
2. Casarone, M.R., Belcaro, G., Nicolaides, A.N., Geroulakos, G., Griffin, M., Incandela, L., De, S.M., Sabetai, M., Geroulakos, G., Agus, G., Bavera, P., Ippolito, E., Leng, G., Di, R.A., Cazaubon, M., Vasdekis, S., Christopoulos, D., and Veller, M. Real epidemiology of varicose veins and chronic venous disease: the San Valentino Vascular Screening Project. Angiology **53,** 2002.
3. Brand, F.N., Dannenberg, A.L., Abbott, R.D., and Kannel, W.B. The epidemiology of varicose veins: the Framingham Study. Am J Prev Med **4,** 96, 1988.
4. Raju, S. Venous insufficiency of the lower limb and stasis ulceration: changing concept and management. Ann Surg **197,** 688, 1983.
5. Pavcnik, D., Uchida, B., Kaufman, J., Hinds, M., Keller, F.S., and Rösch, J. Percutaneous management of chronic deep venous reflux: review of experimental work and early clinical experience with bioprosthetic valve. Vasc Med **13,** 1, 2008.
6. Mayberry, J.C., Moneta, G.L., Taylor, L.M., and Porter, J.M. Fifteen-year results of ambulatory compression therapy for chronic venous ulcers. Surgery **109,** 575, 1991.
7. Zervides, C., and Giannoukas, A.D. Historical overview of venous valve prostheses for the treatment of deep venous valve insufficiency. J Endovasc Ther **19,** 2, 2012.
8. Weber, B., Emmert, M.Y., and Hoerstrup, S.P. Stem cells for heart valve regeneration. Swiss Med Wkly **142,** w13622, 2012.
9. Weber, B., Emmert, M.Y., Schoenauer, R., Brokopp, C., Baumgartner, L., and Hoerstrup, S.P. Tissue engineering on matrix: future of autologous tissue replacement. Semin Immunopathol **33,** 3, 2011.
10. Schmidt, D., Achermann, J., Odermatt, B., Breymann, C., Mol, A., Genoni, M., Zund, G., and Hoerstrup, S.P. Prenatally fabricated autologous human living heart valves based on amniotic fluid derived progenitor cells as single cell source. Circulation **11,** 116, 2007.
11. Mol, A., Rutten, M.C., Driessen, N.J., Bouten, C.V., Zünd, G., Baaijens, F.P., and Hoerstrup, S.P. Autologous human tissue-engineered heart valves: prospects for systemic application. Circulation **4,** 114, 2006.
12. Schmidt, D., Mol, A., Breymann, C., Achermann, J., Odermatt, B., Gössi, M., Neuenschwander, S., Prêtre, R., Genoni, M., Zund, G., and Hoerstrup, S.P. Living autologous heart valves engineered from human prenatally harvested progenitors. Circulation **4,** 114, 2006.
13. Hoerstrup, S.P., Kadner, A., Melnitchouk, S., Trojan, A., Eid, K., Tracy, J., Sodian, R., Visjager, J.F., Kolb, S.A., Grunenfelder, J., Zund, G., and Turina, M.I. Tissue engineering of functional trileaflet heart valves from human marrow stromal cells. Circulation **24,** 106, 2002.
14. Schmidt, D., Dijkman, P.E., Driessen-Mol, A., Stenger, R., Mariani, C., Puolakka, A., Rissanen, M., Deichmann, T., Odermatt, B., Weber, B., Emmert, M.Y., Zund, G., Baaijens, F.P., and Hoerstrup, S.P. Minimally-invasive implantation of living tissue engineered heart valves: a comprehensive approach from autologous vascular cells to stem cells. J Am Coll Cardiol **3,** 56, 2010.
15. Weber, B., Emmert, M.Y., Behr, L., Schoenauer, R., Brokopp, C., Drögemüller, C., Modregger, P., Stampanoni, M., Vats, D., Rudin, M., Bürzle, W., Farine, M., Mazza, E., Frauenfelder, T., Zannettino, A.C., Zünd, G., Kretschmar, O., Falk, V., and Hoerstrup S.P. Prenatally engineered autologous amniotic fluid stem cell-based heart valves in the fetal circulation. Biomaterials **33,** 16, 2012.
16. Weber, B., Scherman, J., Emmert, M.Y., Gruenenfelder, J., Verbeek, R., Bracher, M., Black, M., Kortsmit, J., Franz, T., Schoenauer, R., Baumgartner, L., Brokopp, C., Agarkova, I., Wolint, P., Zund, G., Falk, V., Zilla, P., and Hoerstrup, S.P. Injectable living marrow stromal cell-based autologous tissue engineered heart valves: first experiences with a one-step intervention in primates. Eur Heart J **32,** 22, 2011.
17. Emmert, M.Y., Weber, B., Wolint, P., Behr, L., Sammut, S., Frauenfelder, T., Frese, L., Scherman, J., Brokopp, C.E., Templin, C., Grünenfelder, J., Zünd, G., Falk, V., and Hoerstrup S.P. Stem cell-based transcatheter aortic valve implantation: first experiences in a pre-clinical model. JACC Cardiovasc Interv **5,** 8, 2012.
18. Roh, J.D., Sawh-Martinez, R., Brennan, M.P., Jay, S.M., Devine, L., Rao, D.A., Yi, T., Mirensky, T.L., Nalbandian, A., Udelsman, B., Hibino, N., Shinoka, T., Saltzman, W.M.,

Snyder, E., Kyriakides, T.R., Pober, J.S., and Breuer, C.K. Tissue-engineered vascular grafts transform into mature blood vessels via an inflammation-mediated process of vascular remodeling. Proc Natl Acad Sci U S A **9,** 107, 2010.
19. Weber, B., Schoenauer, R., Papadopulos, F., Modregger, P., Peter, S., Stampanoni, M., Mauri, A., Mazza, E., Gorelik, J., Agarkova, I., Frese, L., Breymann, C., Kretschmar, O., and Hoerstrup, S.P. Engineering of living autologous human umbilical cord cell-based septal occluder membranes using composite PGA-P4HB matrices. Biomaterials **32,** 36, 2011.
20. Cesarone, C.F., Bolognesi, C., and Santi, L. Improved microfluorometric DNA determination in biological material using 33258 Hoechst. Anal Biochem **100,** 1, 1979.
21. Farndale, R.W., Buttle, D.J., and Barrett, A.J. Improved quantitation and discrimination of sulphated glycosaminoglycans by use of dimethylmethylene blue. Biochim Biophys Acta **883,** 2, 1986.
22. Huszar, G., Maiocco, J., and Naftolin, F. Monitoring of collagen and collagen fragments in chromatography of protein mixtures. Anal Biochem **105,** 424, 1980.
23. David, C., Nöhammer, B., Solak, H.H., and Ziegler, E. Differential x-ray phase contrast imaging using a shearing interferometer. Appl Phys Lett **81,** 3287, 2002.
24. Weitkamp, T., Diaz, A., David, C., Pfeiffer, F., Stampanoni, M., and Cloetens, P. X-ray phase imaging with a grating interferometer, Opt Express **13,** 16, 2005.
25. Pfeiffer, F., Bunk, O., David, C., Bech, M., Le Duc, G., Bravin, A., and Cloetens, P. High-resolution brain tumor visualization using three-dimensional x-ray phase contrast tomography. Phys Med Biol **52,** 6923, 2007.
26. McDonald, S.A., Marone, F., Hintermüller, C., Mikuljan, G., David, C., and Pfeiffer, F. Advanced phase-contrast imaging using a grating interferometer. J Synchrotron Radiat **16,** 4, 2009.
27. Modregger, P., Pinzer, B.R., Thüring, T., Rutishauser, S., David, C., and Stampanoni, M. Sensitivity of X-ray grating interferometry. Opt Express **19,** 18324, 2011.
28. Criqui, M.H., Jamosmos, M., Fronek, A., Denenberg, J.O., Langer, R.D., Bergan, J., and Golomb, B.A. Chronic venous disease in an ethnically diverse population: the San Diego Population Study. Am J Epidemiol **158,** 5, 2003.
29. Recek, C. The venous reflect. Angiology **55,** 5, 2004.
30. Taheri, S.A., and Schultz, R.O. Experimental prosthetic vein valve. Long-term results. Angiology. **46,** 4, 1995.
31. Kaya, M., Grogan, J.B., Lentz, D., Tew, W., and Raju, S. Glutaraldehyde-preserved venous valve transplantation in the dog. J Surg Res **45,** 3, 1988.
32. Neglén, P., and Raju, S. Venous reflux repair with cryopreserved vein valves. J Vasc Surg **37,** 3, 2003.
33. Rosenbloom, M.S., Schuler, J.J., Bishara, R.A., Ronan, S.G., and Flanigan, D.P. Early experimental experience with a surgically created, totally autogenous venous valve: a preliminary report. J Vasc Surg **7,** 5, 1988.
34. Dalsing, M.C., Lalka, S.G., Unthank, J.L., Grieshop, R.J., Nixon, C., and Davis, T. Venous valvular insufficiency: influence of a single venous valve (native and experimental). J Vasc Surg **14,** 5, 1991.
35. Plagnol, P., Ciostek, P., Grimaud, J.P., and Prokopowicz, S.C. Autogenous valve reconstruction technique for post-thrombotic reflux. Ann Vasc Surg **13,** 3, 1999.
36. Opie, J.C., Izdebski, T., Payne, D.N., and Opie, S.R. Monocusp—novel common femoral vein monocusp surgery uncorrectable chronic venous insufficiency with aplastic/dysplastic valves. Phlebology **23,** 4, 2008.
37. Teebken, O.E., Puschmann, C., Aper, T., Haverich, A., and Mertsching, H. Tissue-engineered bioprosthetic venous valve: a long-term study in sheep. Eur J Vasc Endovasc Surg **25,** 4, 2003.
38. Llames, S., García, E., Otero, Hernández, J., and Meana, A. Tissue bioengineering and artificial organs. Adv Exp Med Biol **741,** 314, 2012.
39. Rodés-Cabau, J. Transcatheter aortic valve implantation: current and future approaches. Nat Rev Cardiol **15,** 9, 2011.
40. de Borst, G.J., Teijink, J.A., and Patterson, M. A percutaneous approach to deep venous valve insufficiency with a new self-expanding venous frame valve. J Endovasc Ther **10, 341,** 2003.
41. Moll, F. Venous valves for chronic venous insufficiency. Presented at the Inaugural Global Endovascular Forum, London, United Kingdom, 2003.
42. Gale, S.S., Shuman, S., and Beebe, H.G. Percutaneous venous valve bioprosthesis: initial observations. Vasc Endovasc Surg **38,** 221, 2004.
43. Pavcnik, D., Kaufman, J., and Uchida, B. Second-generation percutaneous bioprosthetic valve: a short-term study in sheep. J Vasc Surg **40,** 1223, 2004.
44. Pavcnik, D., Kaufman, J.A., and Uchida, B.T. Significance of spatial orientation of percutaneously placed bioprosthetic venous valves in an ovine model. J Vasc Interv Radiol **16,** 1511, 2005.
45. Pavcnik, D., Yin, Q., and Uchida, B. Percutaneous autologous venous valve transplantation: short-term feasibility study in an ovine model. J Vasc Surg **46,** 338, 2007.
46. Kiefer, P., Gruenwald, F., Kempfert, J., Aupperle, H., Seeburger, J., Mohr, F.W., and Walther, T. Crimping may affect the durability of transcatheter valves: an experimental analysis. Ann Thorac Surg **92,** 1, 2011.
47. Dijkman, P.E., Driessen-Mol, A., Frese, L., Hoerstrup, S.P., and Baaijens, F.P. Decellularized homologous tissue-engineered heart valves as off-the-shelf alternatives to xeno- and homografts. Biomaterials **33,** 18, 2012.

Address correspondence to:
Simon P. Hoerstrup, MD, PhD
Swiss Center of Regenerative Medicine
University Hospital of Zurich
Raemistrasse 100
8091 CH-Zürich
Switzerland

E-mail: simon_philipp.hoerstrup@usz.ch

Received: March 22, 2013
Accepted: October 7, 2013
Online Publication Date: January 17, 2014